

## UV-Radiation and TiO<sub>2</sub> Nanoparticles Effects on Physical Properties of PVA/CMC/TiO<sub>2</sub> Nanocomposite Films

Sara H. Abeam<sup>a\*</sup>, Mahasin F. Hadi Al-Kadhemy<sup>a</sup>, and Khaldoun N. Abbas<sup>a</sup>

<sup>a</sup> Physics Department- Mustansiriyah University-Iraq

\*Corresponding author. Tel.: +0-000-000-0000; fax: +0-000-000-0000; e-mail: hashemsara757@gmail.com

Received 20 February 2023, Revised 1 June 2023, Accepted 21 June 2023

### ABSTRACT

Fabrication of nanocomposite films of polyvinyl alcohol/carboxymethyl cellulose (PVA/CMC) blended with Titanium dioxide nanoparticles (TiO<sub>2</sub> NPs) by a modest solution casting technique is investigated. Also, TiO<sub>2</sub> NPs and UV-irradiation effects for different intervals (12, 26, 40, and 48 hours) on the morphology (FESEM), structure (XRD), composition (FTIR) and optical properties (UV-Vis) of as-prepared films are inspected. FESEM images display that the morphology of PVA/CMC/TiO<sub>2</sub> nanocomposite films is altered due to the strong influence of TiO<sub>2</sub> NPs and UV exposure. The XRD spectra indicate that the amorphous phase of the samples has changed (decline or enhancement) due to UV exposure. The FTIR spectra demonstrate that the UV-irradiation period had a favourable impact on polymer structure by exhibiting some interesting IR peaks. Furthermore, the UV-Vis examination illustrates that the increased UV-irradiation times (12 h to 40 h) and TiO<sub>2</sub> NPs addition improved the absorption intensity of the as-prepared films. Interestingly, the Energy gap  $E_g$  of the nanocomposite films was tuned from 4.47 eV to 5.01 eV with increased irradiation time (12 h to 40 h). In contrast, due to a higher increased UV-irradiation time of 48 h, the Energy gap  $E_g$  value of nanocomposite film was decreased to 4.62 eV. That can be attributed to the strong effect of UV exposure, which influenced the creation of structural defects. Finally, these findings prove that the PVA/CMC/TiO<sub>2</sub> nanocomposite films have an amazing chance to be used in important optoelectronic applications.

**Keywords:** Energy Gap Tuning, PVA/CMC/TiO<sub>2</sub> Nanocomposites Properties, TiO<sub>2</sub> Nanoparticles, UV-Irradiation Time

### 1. INTRODUCTION

Polymers with various optical properties have gained a lot of attention in recent years due to their different applications, such as sensors and light-emitting diodes. Controlling the filler concentrations can easily tune the optical characteristics of these materials. Even though numerous studies have been done on such materials (1). Polyvinyl alcohol (PVA) has gotten a lot of attention from academics because of its good film-forming properties, nontoxicity, low cost, biodegradability, mechanical characteristics, and amazing optical qualities (2). Also, among the cellulose ethers, carboxymethyl cellulose (CMC) in the form of sodium salt is the most extensively utilized. The CMC structure is based on the cellulose polymer 1, 4- $\beta$ -D glucopyranose.

The use of cellulose derivatives has resulted in the development of cellulose-based hydrogels, such as through physical and chemical cross-linking (3). The most often used natural polysaccharide polymer, has excellent biodegradability, biocompatibility, and film-forming properties. Because of its safety and non-toxicity, it is widely utilized in the pharmaceutical, food, and packaging industries (4). Moreover, nanotechnology is a highly effective technology. Nanotechnology is described as the use of structures of at least one-nanometer dimension for the production of materials, electronics, or systems that

have novel or considerably improved qualities as a result of their nanosize (5). TiO<sub>2</sub> nanostructure is an interesting semiconductor. Various processes are used to synthesize TiO<sub>2</sub> nanostructures, the most prevalent of which is single gel processing. It is a versatile transition metal oxide that can be used in a variety of current and future applications, including catalysis, electronics, photonics, sensing, controlled drug release, and medication.

It is a well-studied metal oxide nanoparticle for its UV-blocking properties, due to its efficiency as a short-wavelength light absorber with strong photostability in contrast to other nanoparticles (6). Previous studies show that, due to their high transparency and refractive index in the visible and near-infrared ranges, TiO<sub>2</sub> films are essential optical materials (7). The UV-radiation technique is known for photolysis. Photoinitiator excitation generates reactive radicals that activate subsequent reactions in the polymer mix, enabling cross-linking between the two polymer chains (8). Several studies have been done in this area, such as; B. Jaleh et al., (9) investigated the effect of UV degradation on the optical and surface properties of a polystyrene-TiO<sub>2</sub> nanocomposite. UV-irradiation has been studied for its effect on the optical properties, crystallinity, surface energy, and degradation of PS-TiO<sub>2</sub> nanocomposite. The optical  $E_g$  values were found

to reduce from 4.54 eV in pure PS to 4.45eV for PS-TiO<sub>2</sub> nanocomposite due to UV-irradiation. After 45 hours of UV irradiation, this value is reduced to 3.46. M. R.Khafaga et al., (10) look into the antimicrobial finishing of cotton fabrics using gamma-irradiated CMC/PVA/TiO<sub>2</sub> nanocomposites. Nitric acid was used as a reducing and stabilizing agent in the synthesis of TiO<sub>2</sub> nanoparticles at various concentrations. Gamma irradiation was used on the coated fabrics to create TiO<sub>2</sub> nanoparticles stabilized in cross-linked CMC/PVA hydrogel. A. A. Alhazime et al., (11) study the physical properties tuning of PVA/PEG blend film due to dopant by CuO nanoparticles. The absorption spectra demonstrated a clear relationship between doping concentration and absorption intensity. Various optical metrics were thoroughly explored and found to be directly affected by nanoparticle doping concentrations. In the current study, the effective investigation of UV-irradiation time and TiO<sub>2</sub> nanoparticles incorporation in (PVA/CMC) blends, which have received only slight attention in the literature; is considered a contribution in this area. The scope of this research can be precise under two main ideas; (i) synthesis and characterization of PVA/CMC/TiO<sub>2</sub> nanocomposite-based films, and (ii) Photo-irradiation (UV light) subjected to as-prepared samples.

## 2. THEORETICAL PART

A fraction of the incident light beam that is not reflected by a material surface when it strikes is either absorbed or transmitted through the substance. According to Beer-Lambert Law, the thickness of the materials and how the photons interact with them affect the amount of beam that is absorbed. Equation (1) expresses the connection between the intensity of the incident and transmitted light (12):

$$I = I_0 e^{-\alpha t} \quad (1)$$

Where (I<sub>0</sub>) and (I) are the incident and transmitted light intensities, respectively, (α) is the optical absorption coefficient and (t) is the thickness of the film. Using this relation of the absorbance  $A = \log(I_0/I)$ , the optical absorption coefficient (α) can be computed from the optical absorption spectrum Equation (2)(13).

$$\alpha t = \log\left(\frac{I_0}{I}\right) = 2.303A \quad (2)$$

Moreover, the following equation can be used to calculate the energy band gap. (3) (14).

$$ah\nu = B(h\nu - E_g)^x \quad (3)$$

Where E<sub>g</sub>: is the optical energy band gap; h: is photon energy; B: is a constant, and x: is constant, the allowed and forbidden direct transitions are (1/2, 3/2), respectively, while the allowed and forbidden indirect transitions are (2, 3), respectively.

Scherer's Equation is used to calculate the average crystallite size (D). (4):

$$D = \frac{K\lambda}{\beta \cos\theta} \quad (4)$$

Where k is the shape factor (0.94), λ is the X-ray wavelength (1.5406 Å), β is the full width at half maximum (FWHM), and (θ) is the diffraction angle. From XRD results, the lattice parameters (a and c) were estimated using the relationships shown below (4).

$$\frac{1}{d_{hkl}^2} = \frac{h^2 + k^2}{a^2} + \frac{l^2}{c^2} \quad (5)$$

Where  $d_{hkl}$  is the inter-plane distance using Miller indices for a particular plane (hkl).

## 3. EXPERIMENTAL WORK

The powder form of carboxymethyl cellulose (CMC) was obtained from the UK-based company AVONCHEM, with an average molecular weight of 67000 g/mole. PVA was purchased from Thomas Baker as a powder with an average molecular weight of 14,000 g/mole (produced in India). TiO<sub>2</sub> nanoparticles possessing an average particle size (15.7 nm) are used to prepare PVA/CMC/TiO<sub>2</sub> nanocomposite film (produced in the United States by Materials Pvt. Ltd.). Briefly, by dissolving 0.25 g of each polymer in 17 ml of distilled water, the solution casting process was employed to create a blend of PVA/CMC. TiO<sub>2</sub> NPs powder was utilized in an amount of 0.008 g with 8 ml of distilled water and mixed with a precursor solution of PVA/CMC blend.

To ensure complete dissolution, the precursor solution was magnetically stirred for 24 hours at room temperature. Forming the PVA/CMC/TiO<sub>2</sub> nanocomposite by pouring out the solution in glass plates with a diameter (5 cm) and allowing it to evaporate slowly at room temperature for (4 days) to get a homogeneous film. The thickness of the as-synthesized PVA/CMC/TiO<sub>2</sub> nanocomposite film was found (0.007) μm. Moreover, the as-prepared films were exposed to a digital UV light system (36 watts) with four (9 watts) bulbs made in China. The exposure period was (12, 26, 40, and 48 h). For each irradiation time, the distance of the sample from the lamp remained unchanged. To examine the absorption and transmission spectra in the (200-900) nm wavelength range, a UV-Visible spectrophotometer of type (T70/T80 Series UV/Vis Spectrometer) was used. The composite properties of each film were determined using FTIR spectroscopy (Bruker-Tensor 27 with ATR unit). The samples' thicknesses were measured with a digital micrometre type (Tasha) manufactured in Japan, with a measurement accuracy (0.001) mm and a measurement range (0-150) mm. The structure of as-prepared films was investigated using an entirely computerized X-ray diffractometer (XRD; X' Pert PRO, PANalytical, Netherlands). High-resolution scanning electron microscopy FESEM (ZEISS SIGMA VP Field Emission Scanning Electron) characterized the morphology of the

surface of pure polymers, TiO<sub>2</sub> NPs and PVA/CMC/TiO<sub>2</sub> nanocomposite films.

#### 4. RESULTS AND DISCUSSION

Figures. (1- A, -B and -C) show the XRD patterns of TiO<sub>2</sub> NPs and PVA-CMC/TiO<sub>2</sub> nanocomposite films before and after being subjected to UV-irradiation for 48 h, respectively. XRD peaks at (25.34°, 36.93°, 37.39°, 38.71°, 48.07°, 53.98°, and 55.01°) have been indexed to the hexagonal crystal structure of the TiO<sub>2</sub> NPs as confirmed in Fig. (1-A). It corresponds to the XRD crystal planes (011), (013), (004), (112), (020), (015), and (121), respectively, which were consistent with (JSCD No. (00-021-1272) [15, 16]. The average crystallite size of TiO<sub>2</sub> NPs in the range of (11.9 to 30.4 nm) was estimated from equation (4) and shown in Table (1). Furthermore, a single peak ( $2\theta = 19.59^\circ$ ) was detected in the XRD pattern of PVA/CMC/TiO<sub>2</sub> nanocomposite film before UV-irradiated it as explored in Fig. (1-B). That implies the amorphous structure of the PVA-CMC/TiO<sub>2</sub> nanocomposite film. Figure. (1-C) illustrates the XRD spectrum of PVA/CMC/TiO<sub>2</sub> nanocomposite film after being subjected to UV-irradiated for 48 h. The findings reveal a broad peak at  $2\theta = 19.64^\circ$  with low intensity compared to Figure. (1-B), this result can be attributed to the UV-irradiation effect. That indicates an increase in the amorphous phase and a decrease in the crystallinity of the as-prepared film. These results could be attributed to the increase of UV-irradiation time (48 h) of blend film resulting in an increased disorder and defects level in their structure caused to the lowest degree of crystallinity of film. Which are strongly consistent with the findings of previous studies (9, 15-16). Generally, the two polymers applied in the current investigation showed semi-crystalline materials because of the occurrence of both crystalline and amorphous districts and the broad peak of PVA/CMC/ TiO<sub>2</sub> film can also be related to the crystalline cellulose structure of CMC (9, 16).

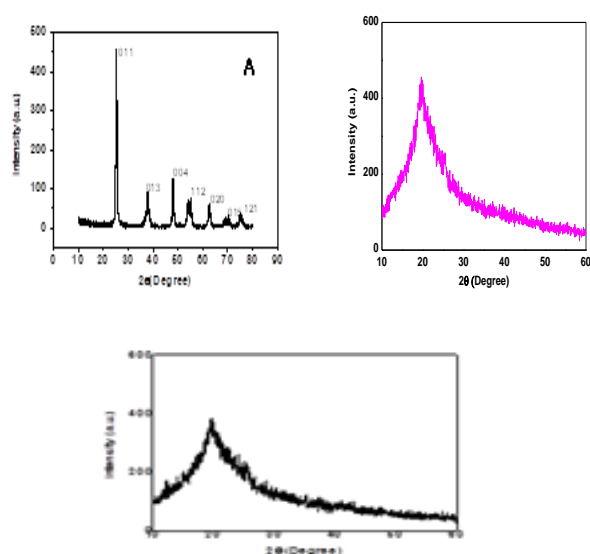
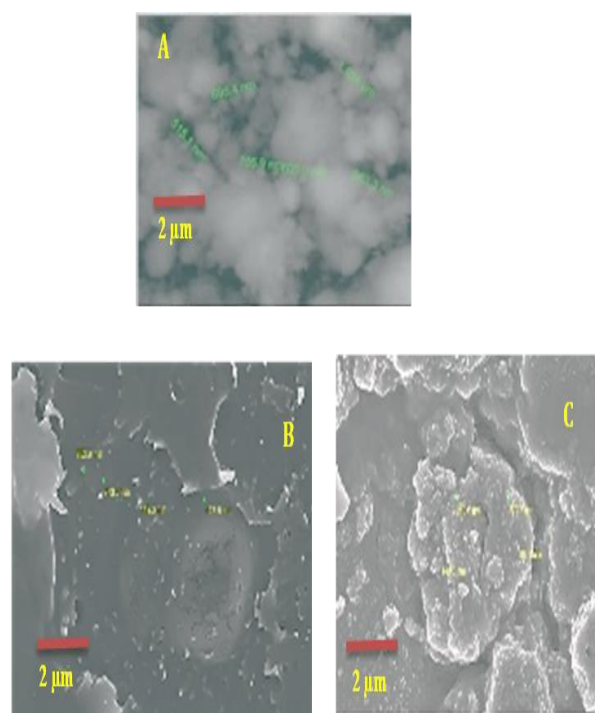


**Figure1** Display the X-ray diffraction patterns of (A) TiO<sub>2</sub> NPs, (B) PVA/CMC/TiO<sub>2</sub> Nanocomposite Film and (C) PVA/CMC/TiO<sub>2</sub> Nanocomposite Film after UV-irradiation for 48 h.

**Table 1** XRD Parameters for TiO<sub>2</sub> NPs

| $2\theta$<br>(deg) | FWHM    | Intensity<br>(counts) | D<br>( $^{\circ}\text{A}$ ) | hkl | D<br>(nm) |
|--------------------|---------|-----------------------|-----------------------------|-----|-----------|
| 25.3424            | 0.54100 | 285                   | 3.51165                     | 011 | 15.1      |
| 36.9362            | 0.28000 | 16                    | 2.43168                     | 013 | 30.4      |
| 37.8804            | 0.67000 | 50                    | 2.37321                     | 004 | 12.6      |
| 38.7148            | 0.50000 | 12                    | 2.32396                     | 112 | 16.9      |
| 48.0716            | 0.59500 | 77                    | 1.89120                     | 020 | 14.7      |
| 53.9815            | 0.75000 | 39                    | 1.69727                     | 015 | 11.9      |
| 55.0311            | 0.73000 | 39                    | 1.66735                     | 121 | 12.2      |

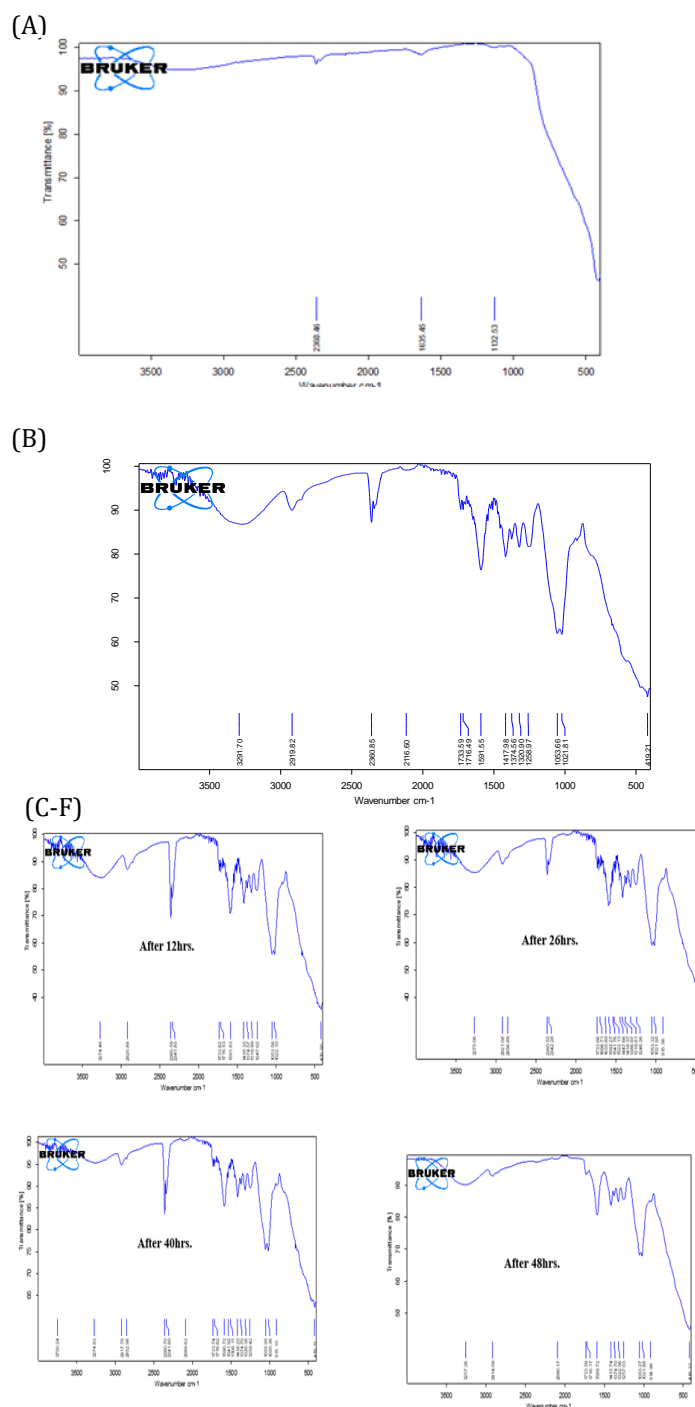
FESEM technique is used to describe the surface morphology of TiO<sub>2</sub> NPs, and PVA/CMC/TiO<sub>2</sub> nanocomposite films before and after UV-irradiation for 48 h as shown in Fig (2 - A, -B and -C), respectively. The FESEM image in Fig (2-A) confirms the formation of TiO<sub>2</sub> NPs possessing the pseudo-spherical shape. From this image, it has been observed that TiO<sub>2</sub> NPs are agglomerated clusters. The FESEM image inspection of the PVA/CMC/TiO<sub>2</sub> nanocomposite film was exposed in an image (2-B), where the surface of the as-prepared sample was aggregates or chunks-like of non-uniform particles before UV-irradiation. Furthermore, the FESEM image in Fig. (2-C) displays the strong effect of the UV-irradiation of PVA/CMC/TiO<sub>2</sub> nanocomposite film; the film shape was changed and seemed like a combination of large and small non-uniform prominent particles. The finding of this FESEM image was strongly consistent with previous studies (7, 17, 18, 19).



**Figures.2** FESEM images for (A) TiO<sub>2</sub> NPs, (B) PVA/CMC/TiO<sub>2</sub> Nanocomposite Film Before UV-Irradiation, and (C) PVA-CMC/TiO<sub>2</sub> Nanocomposite Film after UV-Irradiation for 48 h.

FTIR transmittance spectra compared were shown in Fig. 3 (A-F) for as-synthesized three samples. FTIR spectrum for pure  $\text{TiO}_2$  nanoparticles was shown in Fig. (3-A). A noticeable broad-band was observed between (3800-3000)  $\text{cm}^{-1}$  which was related to the stretching mode of hydroxyl (OH) representing the water moisture. The IR absorption bands at 435, 91  $\text{cm}^{-1}$ , and 466.77  $\text{cm}^{-1}$  to 700  $\text{cm}^{-1}$  illustrate the bending and stretching modes of Ti-O-Ti. These results amazingly matched the results obtained by Jaleh *et al.* (9). Furthermore, FTIR spectrum for PVA/CMC/ $\text{TiO}_2$  nanocomposite film before its UV-irradiated was examined as shown in Fig. (3-B) and Table (2). In this Fig. the IR peaks (3200-3550)  $\text{cm}^{-1}$  and (2920)  $\text{cm}^{-1}$  referred to O-H and C-H stretching modes were assigned to both CMC and PVA polymers, respectively. The O=C=O stretching mode (1340-1360)  $\text{cm}^{-1}$  has distinguished appeared in the composite films. Moreover, the asymmetrical stretching vibration of COO<sup>-</sup> at (1591.55)  $\text{cm}^{-1}$  of the carbonyl group of CMC polymer was observed. The blend films comprised the C=O carbonyl stretch bond (1733.61  $\text{cm}^{-1}$ ) from vinyl alcohol, and acetate groups (PVA polymer). The IR absorption bands located at (1417  $\text{cm}^{-1}$ ), (1300-1461  $\text{cm}^{-1}$ ), and (1050-1300)  $\text{cm}^{-1}$  were assigned to the C-H scissoring and C-H bending as well as C-O stretch of PVA polymer, respectively [4, 19-22]. According to the FTIR analysis results, FTIR spectra confirmed the formation of PVA/CM/ $\text{TiO}_2$  nanocomposite film with slight displacement in the IR peaks. Where both polymers and  $\text{TiO}_2$  NPs were justly physically blended without forming any chemical connections. It has been demonstrated that the embedded  $\text{TiO}_2$  NPs have no effect on the IR spectral characteristics of the polymeric matrix. This strongly supported the previous study's findings. (1, 17, 24, 25). The effect of UV-irradiation on the composition properties of PVA/CM/ $\text{TiO}_2$  nanocomposite films as illustrated in Figs. (3 C-F). The IR absorption bands were specified in Table (2) for different irradiation times (12, 26, 40, and 48 h). Figs. (3 C-F) exhibit that the IR peaks of O-H stretching mode (3200-3550)  $\text{cm}^{-1}$  were noticed for all irradiation times. Some vibrational transitions appeared from 4000 to 3275  $\text{cm}^{-1}$  in (12 and 40 h). The C-H stretching (2920  $\text{cm}^{-1}$ ) refers to both PVA and CMC polymers associated by some shifting in wavenumber. Moreover, the single bond character of the C=O carbonyl stretching absorption (1733.61  $\text{cm}^{-1}$ ) from vinyl alcohol, and acetate groups (PVA polymer) and the bond of C-O stretch (1050-1300)  $\text{cm}^{-1}$  have appeared at all irradiation times. Also, asymmetrical COO<sup>-</sup>-stretching (1591.67  $\text{cm}^{-1}$ ) and C-H scissoring (1300-1461  $\text{cm}^{-1}$ ) of a carbonyl group were observed at all times of irradiation. Significantly, several new IR peaks seemed at (1716.53  $\text{cm}^{-1}$  for 1 h, 1696.71  $\text{cm}^{-1}$ , 1511.76  $\text{cm}^{-1}$ , 1522.13  $\text{cm}^{-1}$  at 26 h, 1716.62  $\text{cm}^{-1}$ , 1590.72  $\text{cm}^{-1}$ , 1506.11  $\text{cm}^{-1}$  at 40 h, and 1716.62  $\text{cm}^{-1}$  and 1589.72  $\text{cm}^{-1}$  at 48 h). The basis of these IR absorption bands was likely due to the UV-radiation exposure of samples.. In addition, at 26 h irradiation time, a new IR peak corresponding to C-H bending 1447.66  $\text{cm}^{-1}$  was performed. The bond of C-C rocking mode was executed for (12, 26, 40, and 48 h). In summary, IR findings of PVA/CMC/ $\text{TiO}_2$  nanocomposite films subjected to UV-irradiation for different times show that the consistent intensities of aforesaid IR peaks (2919, 1416, 1374, 1322, and 1053  $\text{cm}^{-1}$ ) varied with an increase in UV exposure time. Thus, these findings can be explained in terms

of PVA structure, which is made up of parallel chains joined by hydrogen bonds. The UV irradiation of PVA/CMC/ $\text{TiO}_2$  nanocomposite film has a great effect on hydrogen bonding as well as chain order, which means the decrease in intensity of these bands under UV radiation indicates no change in chemical structure. the change was only in the value transmission, and no bond appeared or disappeared. FTIR spectrum for all samples revealed that no chemical interactions were observed between nanoparticles and polymers. So will take physical reaction only.

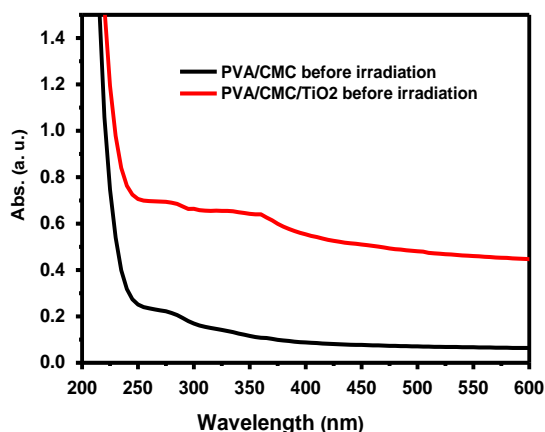


**Figures 3 A-F.** The FTIR spectra of (A)  $\text{TiO}_2$  NPs, (B) PVA/CMC/ $\text{TiO}_2$  nanocomposite films before UV-irradiation and (C-F) after UV-irradiation at different times; 12 h, 26 h, 40h, and 48 h.

**Table 2** FTIR-Characteristic of PVA/CMC/TiO<sub>2</sub> Nanocomposite Film

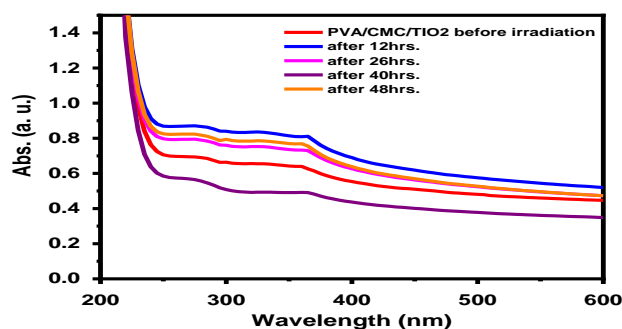
| Assignments                           | Wavenumber (cm <sup>-1</sup> ) |            |           |            |           |
|---------------------------------------|--------------------------------|------------|-----------|------------|-----------|
|                                       | Before UV-irradiation          | After 12h. | After 26h | After 40h. | After 48h |
| <b>O-H Stretching</b>                 | 3257.26                        | 3274.83    | 3275.06   | 3274.48    | 3257.26   |
| <b>C-H stretching</b>                 | 2921.06                        | 2920.88    | 2919.82   | 2917.78    | 2914.09   |
| <b>C-H,CH<sub>2</sub> bending</b>     | 2360.70                        | 2360.55    | 2360.59   | 2360.85    | .....     |
|                                       | 2341.80                        | 2342.28    | 2341.85   | 2116.60    |           |
|                                       | 2069.63                        |            |           |            |           |
| <b>COO- stretching Carbonyl group</b> | 1733.45                        | 1733.99    | 1733.63   | 1733.00    | 1733.59   |
|                                       | 1716.62                        | 1716.66    | 1696.71   | 1716.53    | 1716.49   |
|                                       | 1589.72                        | 1590.09    | 1592.76   | 1591.83    | 1591.55   |
|                                       |                                | 1506.11    | 1522.13   |            |           |
| <b>C-H scissoring</b>                 | 1417.96                        | 1418.35    | 1447.66   | 1418.25    | 1415.74   |
|                                       | 1374.56                        | 1374.57    | 1418.73   | 1374.70    |           |
|                                       |                                |            | 1336.79   |            | 1322.56   |
|                                       | 1320.90                        | 1322.99    | 1319.81   | 1320.38    |           |
| <b>C-O stretch</b>                    | 1257.03                        | 1259.42    | 1246.26   | 1247.02    | 1258.97   |
|                                       | 1053.42                        | 1053.36    | 1053.32   | 1053.56    | 1053.66   |
|                                       | 1021.88                        | 1020.36    | 1021.95   | 1022.10    | 1021.81   |
| <b>1,4-β Glycoside of Cellulose</b>   | 914.96                         | 915.10     | 915.56    | .....      | .....     |

UV-Visible absorbance spectra were studied for PVA/CMC blend film and PVA-CMC/TiO<sub>2</sub> nanocomposite film as shown in Figure (4). It is clear that the UV absorption edge for PVA/CMC film is located at around 245 nm which may be attributed to  $\pi \rightarrow \pi^*$  electronic transition. This finding was consistent the report studies (25-29). Whereas the UV absorption edge of PVA/CMC/TiO<sub>2</sub> nanocomposite film was (260 nm). Overall, there is an essential increase in the light absorption intensity of this film in both regions (UV and Vis) compared to the PVA/CMC blend film spectrum. These results can be related to the addition of TiO<sub>2</sub> NPs to the polymer matrix. This finding was supported by previous studies (4 and 31).



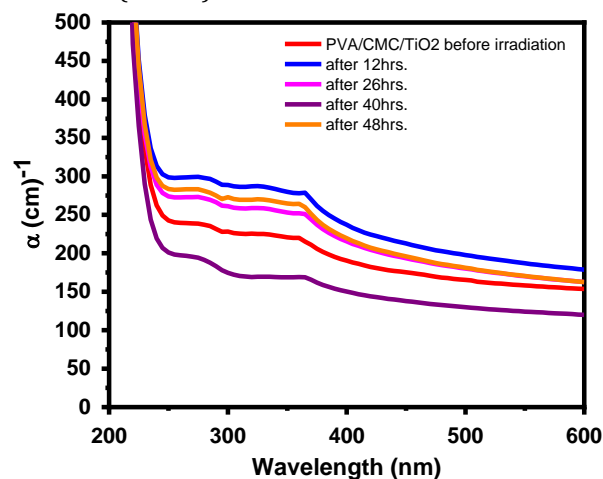
**Figure 4** UV- Vis Absorption spectrum for PVA/CMC/TiO<sub>2</sub> Nanocomposite Films at Different UV-irradiation Times

Figure (5) demonstrates the absorption spectra for PVA/CMC/TiO<sub>2</sub> nanocomposite films before and after UV-irradiation times (12, 26, 40 and 48 h). Figure (5) reveals that the absorption intensity-dependent UV-irradiation time was increased compared to the unirradiated sample. These results were attributed to an increase in the energy of atoms that leads to the increase in the number of collisions between incident atoms, which in turn, leads to decreasing transmittance and increasing absorbance (5, 25, 31). Furthermore, the significant red-shift of the absorption edge towards higher wavelengths (from 260 nm to 280 nm) associated with higher intensity occurred due to an increase in UV-irradiation time. That suggests the UV-irradiation effect led to a decrease in the optical energy band-gap of as-synthesis film due to the creation of defect levels, where the effect of the defects was augmented(18).



**Figure5** UV- Vis Absorption spectrum for PVA/CMC/TiO<sub>2</sub> Nanocomposite Films at Different UV-irradiation Times

Furthermore, the absorption coefficient ( $\alpha$ ) of all samples was estimated by using Equation. (2) as presented in Fig (6). It refers to the capacity of a material to absorb light with a specific wavelength per unit length. Overall, if the value of the absorption coefficient was less than ( $\alpha < 104 \text{ cm}^{-1}$ ) that means the indirect electronic transition occurred (32- 34).



**Figure 6** UV-Vis Absorption Coefficient for PVA/CMC/TiO<sub>2</sub> Nanocomposite Films at Different UV-irradiation Times

Figure (7) displays the optical energy band gap ( $E_g$ ) for PVA/CMC/TiO<sub>2</sub> nanocomposite films before and after UV-irradiation. The result indicate that the UV-irradiation time (12 to 40 h) led to an increase in the  $E_g$  of films (4.47 - 5.01 eV) as demonstrated by (Table 3). Additionally, the increase of UV-irradiation time to 48 h caused a decrease in the  $E_g$  of the film, which may be clarified as a result of increasing the disorder degree because of the generated new defect levels in the band-gap of the nanocomposite film, which promotes an  $E_g$  narrowing (8, 25,30-32).

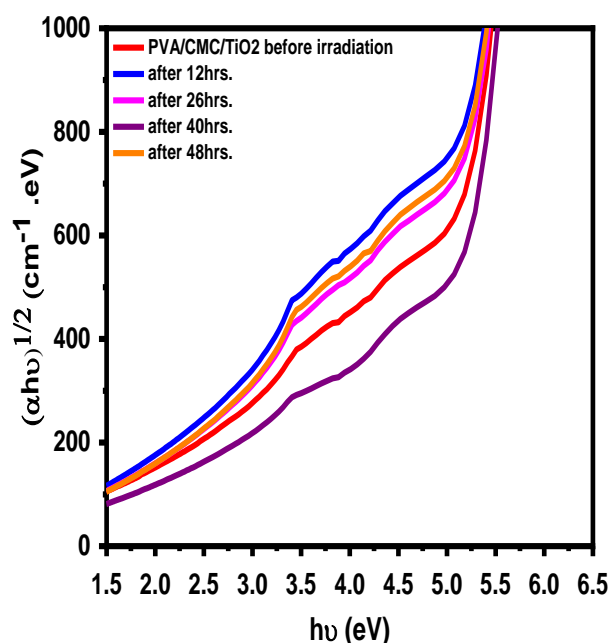


**Figure7** UV-Vis Optical energy gap for PVA/CMC/TiO<sub>2</sub> Nanocomposite Films at Different UV-irradiation Times

**Table 3** Energy band gap value of PVA/CMC/TiO<sub>2</sub> Nanocomposite Films

| $E_g$ (eV) | UV-irradiation times (h) |
|------------|--------------------------|
| 4.82       | 0                        |
| 4.47       | 12                       |
| 4.74       | 26                       |
| 5.01       | 40                       |
| 4.62       | 48                       |

## 5. CONCLUSION

The synthesized PVA/CMC/TiO<sub>2</sub> nanocomposite film via the simple solution casting route as well as the effect of UV-irradiation time on the as-prepared films were investigated. The XRD data reveal that UV-irradiation time changes the structure quality of samples by enhancing their amorphous nature. The FESEM image results of blend films show an interesting modification in the morphology of nanocomposite films dependent on UV irradiation. The FTIR spectrum revealed that TiO<sub>2</sub> and UV exposure had a positive effect on the polymer structure by forming covalent connections between PVA and CMC. Finally, the UV-Vis examination demonstrates that the absorption intensity of nanocomposite films was increased due to the strong effect of TiO<sub>2</sub> NPs and UV irradiation. The change (increase and decrease) in the optical band gap-dependent UV-irradiation time of films was observed, which makes them a strong candidate for optoelectronic applications.

## ACKNOWLEDGMENTS

The authors would like to thank Mustansiriyah University ([www.uomustansiriyah.edu.iq](http://www.uomustansiriyah.edu.iq)) Baghdad-Iraq for its support in the present work.

## REFERENCES

- [1] V. S. Sangawar and M. C. Golchha, "Evolution of the optical properties of Polystyrene thin films filled with Zinc Oxide nanoparticles," *Int. J. Sci. Eng. Res.*, vol. 4, no. 6.
- [2] M. M. Rahman Khan *et al.*, "Synthesis, Luminescence and Thermal Properties of PVA-ZnO-Al<sub>2</sub>O<sub>3</sub> Composite Films: Towards Fabrication of Sunlight-Induced Catalyst for Organic Dye Removal," *J. Polym. Environ.*, vol. 26, no. 8, pp. 3371-3381, 2018.
- [3] S. Villaruel *et al.*, "Changes induced by UV radiation in the presence of sodium benzoate in films formulated with polyvinyl alcohol and carboxymethyl cellulose," *Mater. Sci. Eng. C*, vol. 56, pp. 545-554, 2015.
- [4] Y. M. Jawad, M. F. H. Al-Kadhemy, and J. A. S. Salman, "Synthesis structural and optical properties of CMC/MgO nanocomposites," *Mater. Sci. Forum*, vol. 1039 MSF (July), pp. 104-114, 2021.
- [5] H. E. Ali, A. Atta, and M. M. Senna, "Physico-Chemical Properties of Carboxymethyl Cellulose

- (CMC)/Nanosized Titanium Oxide (TiO<sub>2</sub>) Gamma Irradiated Composite," *Arab J. Nucl. Sci. Appl.*, vol. 48, no. 4, pp. 44–52, 2015.
- [6] T. G. Hoffmann *et al.*, "Potentials nanocomposites in food packaging," *Chem. Eng. Trans.*, vol. 75 (June), pp. 253–258, 2019.
- [7] C. Ye *et al.*, "Optical properties of MgO-Ti O<sub>2</sub> amorphous composite films," *J. Appl. Phys.*, vol. 102, no. 1, 2007.
- [8] S. Villarruel *et al.*, "Changes induced by UV radiation in the presence of sodium benzoate in films formulated with polyvinyl alcohol and carboxymethyl cellulose," *Mater. Sci. Eng. C*, vol. 56, pp. 545–554, 2015.
- [9] B. Jaleh *et al.*, "UV-degradation effect on optical and surface properties of polystyrene-TiO<sub>2</sub> nanocomposite film," *J. Iran. Chem. Soc.*, vol. 8 (SUPPL. 1), pp. 161–168, 2011.
- [10] M. R. Khafaga, H. E. Ali, and A. W. M. El-Naggar, "Antimicrobial finishing of cotton fabrics based on gamma irradiated carboxymethyl cellulose/poly(vinyl alcohol)/TiO<sub>2</sub> nanocomposites," *J. Textile Inst.*, vol. 107, no. 6, pp. 766–773, 2016.
- [11] A. A. Alhazime, "Effect of Nano CuO Doping on Structural, Thermal and Optical Properties of PVA/PEG Blend," *J. Inorg. Organomet. Polym. Mater.*, 2020.
- [12] K. H. H. Al-Attayah, A. Hashim, and S. F. Obaid, "Fabrication of novel (carboxy methyl cellulose-polyvinylpyrrolidone-polyvinyl alcohol)/lead oxide nanoparticles: structural and optical properties for gamma rays shielding applications," *Int. J. Plast. Technol.*, vol. 23, no. 1, pp. 39–45, 2019.
- [13] A. Hadi and A. Hashim, "Development of a new humidity sensor based on (Carboxymethyl cellulose-starch) blend with copper oxide nanoparticles," *Ukr. J. Phys.*, vol. 62, no. 12, pp. 1044–1049, 2017.
- [14] N. R. Dhineshababu, R. Vettumperumal, and R. Kokila, "A study of linear optical properties of ternary blends PVA/CMC/aloe vera biofilm for UV shielding," *Appl. Nanosci.*, vol. 11, no. 2, pp. 669–678, 2021.
- [15] A. S. Abouhaswa, G. M. Turky, and T. S. Soliman, "Nd:YAG nanosecond laser induced growth of Au nanoparticles within CMC/PVA matrix: Multifunctional nanocomposites with tunable optical and electrical properties," *Compos. Commun.*, vol. 24, p. 100662, January 2021.
- [16] S. A. Madhloom, "Structural Properties of Nanoparticles TiO<sub>2</sub>/PVA Polymeric Films," *Al-Mustansiriyah J. Sci.*, vol. 28, no. 2, pp. 188–195, 2018.
- [17] C. A. Duarte *et al.*, "Characterization of Crystalline Phase of TiO<sub>2</sub>," *Materials*, vol. 13, p. 4071, 2020.
- [18] P. A. Putro, N. Yudasari, and A. Maddu, "Spectroscopic Study on the Film of Polyvinyl Alcohol and Carboxymethyl Cellulose as Polymer Electrolyte Materials," *J. Phys.: Conf. Ser.*, vol. 1491, no. 1, 2020.
- [19] M. Abbas, M. Abdallah, and T. Alwan, "Optical characterization of nickel doped poly vinyl alcohol films," *SOP Trans. Phys. Chem.*, vol. 1, no. 2, pp. 1–9, 2014.
- [20] N. V. Bhat *et al.*, "Effect of  $\gamma$ -radiation on the structure and morphology of polyvinyl alcohol films," *Nucl. Instrum. Methods Phys. Res. B*, vol. 237, nos. 3–4, pp. 585–592, 2005.
- [21] A. Kharazmi *et al.*, "Structural, optical, opto-thermal and thermal properties of ZnS-PVA nanofluids synthesized through a radiolytic approach," *Beilstein J. Nanotechnol.*, vol. 6, no. 1, pp. 529–536, 2015.
- [22] S. Hashem, M. Fadhil, and K. Najji, "Study Physical Characteristics of Polyvinyl Alcohol/Carboxymethyl cellulose Blend Films," *55(393)*, pp. 298–305, 2022.
- [23] M. El-Sakhawy *et al.*, "Preparation and infrared study of cellulose based amphiphilic materials," *Cellulose Chem. Technol.*, vol. 52, nos. 3–4, pp. 193–200, 2018.
- [24] C. Films, "Effects of Raw Material Source on the Properties of CMC," pp. 1–15, 2022.
- [25] N. T. T. Thuy *et al.*, "Green synthesis of silver nanoparticles using plectranthus amboinicus leaf extract for preparation of cmc/pva nanocomposite film," *J. Renewable Mater.*, vol. 9, no. 8, pp. 1393–1411, 2021.
- [26] M. Behera, "An intensive study on the optical, rheological, and electrokinetic properties of polyvinyl alcohol-capped nanogold," *Int. Nano Lett.*, vol. 5, no. 3, pp. 161–169, 2015.
- [27] M. F. H. Al-Kadhemy, S. A. Ibrahim, and J. A. S. Salman, "Studying the physical properties polyvinyl alcohol polymer mixture with silica nanoparticles and its application as pathogenic bacteria inhibitor," *AIP Conf. Proc.*, vol. 2290, 2020.
- [28] A. H. Mohammad, H. A. Yasser, and A. H. Hassan, "Optical Properties of PolyVinyl Alcohol with Phenol," *J. Coll. Educ.*, vol. 3, pp. 91–102, 2015.
- [29] N. H. El Fewaty, A. M. El Sayed, and R. S. Hafez, "Synthesis, structural and optical properties of tin oxide nanoparticles and its CMC/PEG-PVA nanocomposite films," *Polym. Sci. Ser. A*, vol. 58, no. 6, pp. 1004–1016, 2016.
- [30] A. F. Saleh *et al.*, "Effect Adding PVA Polymer on Structural and Optical Properties of TiO<sub>2</sub> Thin Films," *17(2)*, pp. 116–121, 2014.
- [31] A. M. Youssef *et al.*, "Development and Characterization of CMC/PVA Films Loaded with ZnO-Nanoparticles for Antimicrobial Packaging Application," *9(9)*, pp. 157–163, 2017.
- [32] G. A. H. Abdul Jabbar, A. A. Saeed, and M. F. H. AL-Kadhemy, "Impact of ZnO Nanoparticle on the Structural and Optical Properties of Poly(vinyl alcohol) Film," *Al-Mustansiriyah J. Sci.*, vol. 33, no. 4, pp. 153–161, 2022.
- [33] Y. M. Jawad *et al.*, "Study the Effect of the Incorporation of Silicon Dioxide Nanoparticles on Improved Performance of Carboxymethyl Cellulose Physical Characteristics," *AIP Conf. Proc.*, vol. 2398, October 2022.
- [34] N. A. Darweesh, A. A. Saeed, and M. F. A.-Kadhemy, "Influence of Weathering on Physical Properties and Sun Light Transmitted through PMMA/Safranin Films for Greenhouse Applications," *1(1)*, pp. 40–53, 2023.